J|A|C|S
ARTICLES
Published on Web 04/25/2007

Properties of Prussian Blue Materials Manifested in Molecular Complexes: Observation of Cyanide Linkage Isomerism and Spin-Crossover Behavior in Pentanuclear Cyanide Clusters

Mikhail Shatruk,[†] Alina Dragulescu-Andrasi,[‡] Kristen E. Chambers,[†] Sebastian A. Stoian,[‡] Emile L. Bominaar,[‡] Catalina Achim,*[,‡] and Kim R. Dunbar*[,†]

Contribution from the Department of Chemistry, Texas A&M University, College Station, Texas 77842-3012, and Department of Chemistry, Carnegie Mellon University, 4400 Fifth Avenue, Pittsburgh, Pennsylvania 15213

Received August 29, 2006; E-mail: dunbar@mail.chem.tamu.edu; achim@cmu.edu

Abstract: Pentanuclear, cyanide-bridged clusters $[M(tmphen)_2]_3[M'(CN)_6]_2$ (M/M′ = Zn/Cr (**1**), Zn/Fe (**2**), Fe/Fe (**3**), Fe/Co (**4**), and Fe/Cr (**5**); tmphen = 3,4,7,8-tetramethyl-1,10-phenanthroline) were prepared by combining $[M'^{III}(CN)_6]^{3-}$ anions with mononuclear complexes of M^{II} ions with two capping tmphen ligands. The clusters consist of a trigonal bipyramidal (TBP) core with three M^{II} ions in the equatorial positions and two M'^{III} ions in the axial positions. Compounds **1**−**4** are isostructural and crystallize in the monoclinic space group $P2_1/c$. Complex **5** crystallizes in the enantiomorphic space group $P3_221$. The magnetic properties of compounds **1** and **2** reflect the contributions of the individual $[Cr^{III}(CN)_6]^{3-}$ and $[Fe^{III}(CN)_6]^{3-}$ ions. The Fe^{II} ions in compounds **3** and **4** exhibit a gradual, temperature-induced spin transition between high spin (HS) and low spin (LS), as determined by the combination of Mössbauer spectroscopy, magnetic measurements, and single-crystal X-ray studies. The investigation of compound **5** by these methods and by IR spectroscopy indicates that cyanide linkage isomerism occurs during cluster formation. The magnetic behavior of **5** is determined by weak ferromagnetic coupling between the axial Cr^{III} centers mediated by the equatorial diamagnetic Fe^{II} ions. Mössbauer spectra collected in the presence of a high applied field have allowed, for the first time, the direct experimental observation of uncompensated spin density at diamagnetic metal ions that bridge paramagnetic metal ions.

Introduction

Since its accidental discovery by the German artist Diesbach in 1703,[1] the compound ferric ferrocyanide $Fe_4[Fe(CN)_6]_3$, commonly known as Prussian blue (PB), has the distinction of being the first material based on molecular coordination compounds. Although PB has been used extensively as a pigment for three centuries and studied half a century ago vis-à-vis its structural, electronic, and magnetic properties,[2−7] a renaissance of chemistry of PB and its transition metal analogues has occurred in the past decade because of the exciting findings that cyanide materials behave as high-temperature molecular magnets,[8−10] photoswitchable magnetic solids,[11] antidotes for radioactive poisoning,[12] molecular sieves,[13] and hydrogen storage materials.[14,15] The variety of interesting properties notwithstanding, it is an ongoing challenge to establish the precise composition of these coordination compounds, given the presence of statistically disordered vacancies in the transition-metal sites, a situation which necessitates the modeling of the geometry around the metal ions by taking into account statistically averaged coordination environments.[7] Given these issues, it is important to design cyanide complexes that manifest, at the molecular level, the fascinating properties exhibited by PB and its analogues. The establishment of structure−property relationships for such complexes as well as their theoretical treatment is facilitated by the fact that the structure is finite and the metal coordination environment is well defined.

The synthesis of such molecular compounds involves the use of multidentate organic ligands that are capable of blocking a specific number of coordination sites on the transition metal ions, thereby preventing the formation of infinite structures.[16] Our efforts in this vein have produced a series of discrete cyano-bridged pentanuclear clusters with a trigonal bipyramidal (TBP) core that exhibit diverse and interesting properties. For example,

[†] Texas A&M University.
[‡] Carnegie Mellon University.

(1) Woodward, J. *Philos. Trans.* **1724**, *33*, 15−17.
(2) Robin, M. B. *Inorg. Chem.* **1962**, *1*, 337−342.
(3) Sano, H.; Hashimoto, F. *Bull. Chem. Soc. Jpn.* **1965**, *38*, 684−685.
(4) Walker, R. G.; Watkins, K. O. *Inorg. Chem.* **1968**, *7*, 885−888.
(5) Ito, A.; Suenaga, M.; Ono, K. *J. Chem. Phys.* **1968**, *48*, 3597−3599.
(6) Mayoh, B.; Day, P. *J. Chem. Soc., Dalton Trans.* **1976**, 1483−1486.
(7) Buser, H. J.; Schwarzenbach, D.; Petter, W.; Ludi, A. *Inorg. Chem.* **1977**, *16*, 2704−2710.
(8) Ferlay, S.; Mallah, T.; Ouahès, R.; Veillet, P.; Verdaguer, M. *Nature* **1995**, *378*, 701−703.
(9) Entley, W. R.; Girolami, G. S. *Science* **1995**, *268*, 397−400.
(10) Holmes, S. M.; Girolami, G. S. *J. Am. Chem. Soc.* **1999**, *121*, 5593−5594.
(11) Sato, O.; Iyoda, T.; Fujishima, A.; Hashimoto, K. *Science* **1996**, *272*, 704−705.
(12) See, for example, http://www.fda.gov/cder/drug/infopage/prussian_blue/.
(13) Boxhoorn, G.; Moolhuysen, J.; Coolegem, J. G. F.; Van Santen, R. A. *J. Chem. Soc., Chem. Commun.* **1985**, 1305−1307.
(14) Chapman, K. W.; Southon, P. D.; Weeks, C. L.; Kepert, C. J. *Chem. Commun.* **2005**, 3322−3324.
(15) Kaye, S. S.; Long, J. R. *J. Am. Chem. Soc.* **2005**, *127*, 6506−6507.
(16) Dunbar, K. R.; Heintz, R. A. *Prog. Inorg. Chem.* **1997**, *45*, 283−391.

10.1021/ja066273x CCC: $37.00

Scheme 1. A TBP Cluster with the Coordination Environment of One Equatorial Metal Ion Identified in Color

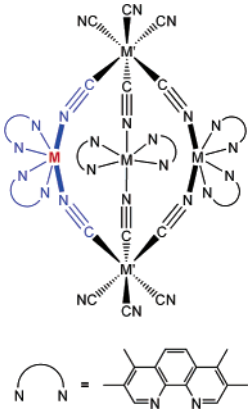

$[Mn^{II}(tmphen)_2]_3[Mn^{III}(CN)_6]_2$ (tmphen = 3,4,7,8-tetramethyl-1,10-phenanthroline) behaves as a single-molecule magnet,[17] and the isostructural compound $[Co^{II}(tmphen)_2]_3[Fe^{III}(CN)_6]_2$[18,19] undergoes a charge-transfer-induced spin transition reminiscent of the behavior observed for the 3-D $Co^{II}-Fe^{III}$ analogue of Prussian blue.[11]

It is noteworthy that the coordination environment of the metal ions situated in the equatorial sites of the TBP clusters consists of two chelating diimine type ligands and two N-bound cyanide ligands (Scheme 1). Given that Fe^{II} complexes with N donor ligands often exhibit spin crossover behavior,[20−23] we introduced Fe^{II} ions into the equatorial position of TBP clusters. The spin crossover phenomenon has been studied extensively over the last 50 years,[24] and it is generally known that interactions between individual spin crossover molecules in crystals mediated by hydrogen bonding or $\pi-\pi$ interactions lead to cooperative behavior, abrupt spin transitions, and thermal hysteresis or bistability within a finite temperature range.[25] The latter property renders spin crossover compounds attractive materials for the development of magnetic sensors and memory devices. Multinuclear spin crossover clusters fall naturally into the regime intermediate between mononuclear complexes and extended solids and can be used to understand the factors that govern cooperativity in spin transitions in solids. Although various dinuclear spin crossover complexes have been described in the literature over the years,[26] there are few reports of spin crossover behavior for clusters of higher nuclearity.[27,28]

Herein we describe the preparation of a series of TBP cyanide-bridged complexes containing Fe^{II} ions in the equatorial positions. The physical properties of these pentanuclear clusters have been found to mimic properties already measured for PB and its analogues. In particular, we have observed cyanide linkage isomerism and a thermally induced transition from the high spin (HS) to the low spin (LS) state of Fe^{II}. We describe and discuss the behavior of these novel compounds and outline further developments that can be pursued based on our recent findings.

Experimental

Starting Materials. The starting materials $K_3[Cr(CN)_6]$ (Aldrich), $K_3[Co(CN)_6]$ (Pfaltz & Bauer), $(TBA)_3[Fe(CN)_6]$ (TBA = tetrabutylammonium; Fluka), anhydrous $FeCl_2$ (Strem), $Zn(NO_3)_2\cdot 6H_2O$ (Fisher), 18-crown-6 (Aldrich), and 3,4,7,8-tetramethyl-1,10-phenanthroline (tmphen; Lancaster) were used as received. Acetonitrile was dried over 3 Å molecular sieves and distilled prior to use. While compounds **1** and **2** were prepared aerobically, **3**, **4**, and **5** were prepared under anaerobic conditions in an N_2-filled dry box. Concentrations of the reactants given below were found to produce the best quality single crystals for structure determination by X-ray crystallography. All of the reactions, however, can be scaled up to obtain products in larger quantities.

$[Zn(tmphen)_2]_3[Cr(CN)_6]_2$ (1). A solution of $[(18\text{-crown-6})K]_3[Cr(CN)_6]$ was prepared by stirring 62.5 mg (0.192 mmol) of $K_3[Cr(CN)_6]$ and 127 mg (0.480 mmol) of 18-crown-6 in 40 mL of acetonitrile for 24 h. The resulting solution was filtered to remove excess $K_3[Cr(CN)_6]$. A second solution was prepared by stirring 47.3 mg (0.159 mmol) of $Zn(NO_3)_2\cdot 6H_2O$ with 76.7 mg (0.325 mmol) of tmphen in 40 mL of acetonitrile to give a clear, colorless solution in 30 min. The two aforementioned solutions were quickly combined in a 100-mL Erlenmeyer flask, and the mixture was left undisturbed for 2 days after which time clear colorless needle-like crystals had formed at the bottom of the flask. The crystals were collected by filtration, washed with acetonitrile (3 × 40 mL), and dried in vacuo. Yield = 96.3 mg (82%). Elemental analysis indicated the presence of interstitial water molecules. Anal. Calcd for $Zn_3Cr_2O_{11}N_{24}C_{108}H_{118}$ (**1**·$11H_2O$): O, 7.90; N, 15.09; C, 58.21; H, 5.34. Found: O, 7.47; N, 14.83; C, 57.09; H, 5.28%.

$[Zn(tmphen)_2]_3[Fe(CN)_6]_2$ (2). Compound **2** was prepared in a fashion analogous to that described above for compound **1**, with the acetonitrile soluble $(TBA)_3[Fe(CN)_6]$ salt (150 mg per 40 mL of solvent) being used as the source of $[Fe(CN)_6]^{3-}$ anions. Yield = 87.2 mg (73%). Elemental analysis indicated the presence of interstitial water molecules. Anal. Calcd for $Zn_3Fe_2O_{12}N_{24}C_{108}H_{120}$ (**2**·$12H_2O$): O, 8.52; N, 14.91; C, 57.55; H, 5.37. Found: O, 8.39; N, 14.66; C, 56.71; H, 4.97%.

$[Fe(tmphen)_2]_3[Fe(CN)_6]_2$ (3). Samples of $FeCl_2$ (20.3 mg, 0.160 mmol) and tmphen (75.7 mg, 0.320 mmol) were combined in 40 mL of acetonitrile, and the solution was stirred for 30 min. The resulting clear dark-red solution was quickly combined with a solution of 150 mg (0.160 mmol) of $(TBA)_3[Fe(CN)_6]$ in 40 mL of acetonitrile in a 100 mL Erlenmeyer flask. The mixture was left undisturbed for 4−5 days. After this period of time, a crop of burgundy red crystals was collected by filtration, washed with acetonitrile (3 × 100 mL), and dried in vacuo. Yield = 41.1 mg (35%). Elemental analysis indicated the presence of interstitial water molecules. Anal. Calcd for $Fe_5O_{14}N_{24}C_{108}H_{124}$ (**3**·$14H_2O$): O, 9.90; N, 14.86; C, 57.36; H, 5.53. Found: O, 10.10; N, 14.79; C, 56.89; H, 5.48%.

$[Fe(tmphen)_2]_3[M'(CN)_6]_2$ (M′ = Co (4), Cr (5)). Compounds **4** and **5** were prepared in a fashion analogous to that described above for compound **3**, and were both obtained as burgundy red crystals. $K_3[Co(CN)_6]$ and $K_3[Cr(CN)_6]$ were made to be soluble in acetonitrile by complexation with 18-crown-6, as described above for compound **1**. Yields = 38.4 mg (32%, **4**) and 59.2 mg (37%, **5**). Elemental analyses

(17) Berlinguette, C. P.; Vaughn, D.; Cañada-Vilalta, C.; Galán-Mascarós, J. R.; Dunbar, K. R. *Angew. Chem., Int. Ed.* **2003**, *42*, 1523−1526.
(18) Berlinguette, C. P.; Dragulescu-Andrasi, A.; Sieber, A.; Galán-Mascarós, J. R.; Güdel, H. U.; Achim, C.; Dunbar, K. R. *J. Am. Chem. Soc.* **2004**, *126*, 6222−6223.
(19) Berlinguette, C. P.; Dragulescu-Andrasi, A.; Sieber, A.; Güdel, H. U.; Achim, C.; Dunbar, K. R. *J. Am. Chem. Soc.* **2005**, *127*, 6766−6779.
(20) König, E.; Madeja, K. *Chem. Commun.* **1966**, 61−62.
(21) Moliner, N.; Gaspar, A. B.; Muñoz, M. C.; Niel, V.; Cano, J.; Real, J. A. *Inorg. Chem.* **2001**, *40*, 3986−3991.
(22) Edwards, M. P.; Hoff, C.; Curnutte, B.; Eck, J. S.; Purcell, K. F. *Inorg. Chem.* **1984**, *23*, 2613−2619.
(23) Kunkeler, P. J.; van Koningsbruggen, P. J.; Cornelissen, J. P.; van der Horst, A. N.; van der Kraan, A. M.; Spek, A. L.; Haasnoot, J. G.; Reedijk, J. *J. Am. Chem. Soc.* **1996**, *118*, 2190−2197.
(24) Gütlich, P.; Goodwin, H. A. *Top. Curr. Chem.* **2004**, *233*, 1−47.
(25) Murray, K. S.; Kepert, C. J. *Top. Curr. Chem.* **2004**, *233*, 195−228.
(26) Real, J. A.; Gaspar, A. B.; Muñoz, M. C.; Gütlich, P.; Ksenofontov, V.; Spiering, H. *Top. Curr. Chem.* **2004**, *233*, 167−193.
(27) Vos, G.; De Graaff, R. A. G.; Haasnoot, J. G.; van der Kraan, A. M.; De, Vaal, P.; Reedijk, J. *Inorg. Chem.* **1984**, *23*, 2905−2910.
(28) (a) Breuning, E.; Ruben, M.; Lehn, J. M.; Renz, F.; Garcia, Y.; Ksenofontov, V.; Gütlich, P.; Wegelius, E.; Rissanen, K. *Angew. Chem., Int. Ed.* **2000**, *39*, 2504−2507. (b) Nihei, M.; Yi, M.; Yokota, M.; Han, L.; Maeda, A.; Kishida, H.; Okamoto, H.; Oshio, H. *Angew. Chem., Int. Ed.* **2005**, *44*, 6484−6487.

are in accord with the presence of interstitial water molecules. Anal. Calcd for $Fe_3Co_2O_{13}N_{24}C_{108}H_{122}$ (**4**·13H_2O): O, 9.25; N, 14.94; C, 57.66; H, 5.47. Found: O, 9.13; N, 14.84; C, 57.60; H, 5.33. Anal. Calcd for $Fe_3Cr_2O_{12}N_{24}C_{108}H_{120}$ (**5**·12H_2O): O, 8.66; N, 15.16; C, 58.49; H, 5.45. Found: O, 8.30; N, 15.00; C, 58.18; H, 5.06.

Physical Measurements. In the study of complexes **3** and **4**, we have discovered a dependence of their properties on the type and amount of solvent present in the crystals. Crystals of these compounds grow from acetonitrile solution and contain interstitial acetonitrile molecules, as determined by X-ray crystallography. Upon removal of the crystals from the mother liquor and their exposure to the lab atmosphere, exchange of the acetonitrile with water takes place. Elemental analysis indicates that after 1−2 days of exposure to air, the sample contains exclusively water, within the precision of this analysis. To study materials whose composition is as defined as possible, we used for Mössbauer spectroscopy and magnetic susceptibility experiments crystals that were washed several times with acetonitrile by decantation, but were kept covered with acetonitrile at all times to avoid solvent exchange. These crystals are referred to as "acetonitrile-wet crystals". We have also studied crystals that were filtered off from the mother liquor, washed with acetonitrile, dried in vacuum, and kept in the lab atmosphere. As shown by elemental analysis, these crystals contain water as crystallization solvent instead of acetonitrile. We refer to these crystals as "water-containing crystals".

The thermogravimetric analyses (TGAs) were performed on a Shimadzu TGA-50 thermogravimetric analyzer in the 298−573 K temperature range at the heating rate of 10 K/min, under an N_2 gas flow of 20 L/min. Infrared (IR) spectra of compounds **1**−**5** were measured as Nujol mulls placed between KBr plates on a Nicolet 740 FTIR spectrometer. Electrospray mass spectrograms were acquired on a MDS Sciex API QStar Pulsar mass spectrometer using an electrospray ionization source. All spectrograms were acquired in the positive ion mode in an acetonitrile/methanol (1:1 v/v) solution of ∼50 μM analyte concentration. The spray voltage was ∼4800 V, and the nozzle skimmer potential was adjusted to 10 V to minimize fragmentation.

Magnetic measurements were performed on a Quantum Design SQUID, MPMS-XL magnetometer. Magnetic susceptibility measurements in the DC mode were carried out in an applied field of 0.1 T in the 2−300 K range. Magnetization data were acquired at 1.8 K with the magnetic field varying from 0 to 7 T. Whenever appropriate, the theoretical simulation of magnetic behavior of the studied complexes was carried out with MAGPACK.[30] Magnetic data obtained for water-containing samples of **1**−**5** were corrected for diamagnetic contributions by the use of the Pascal constants.[29] Because of the high content of disordered solvent in the crystals, immediately after being studied by magnetic susceptibility, each sample was subject to TGA. The molecular weight of each compound was adjusted according to the interstitial solvent content determined from the TGA. Each sample was also characterized by IR spectroscopy and elemental analysis.

The magnetic properties of compounds **3** and **4** were also measured on acetonitrile-wet crystals sealed in a 4-mm NMR tube. The data obtained for these samples were corrected for the diamagnetic contributions from the solvent and the NMR tube, as well as for the diamagnetic contribution of the compound itself.

The ^{57}Fe Mössbauer spectra were collected on constant acceleration instruments over the temperature range of 1.5−300 K, in applied external fields up to 8 T. Samples for experiments in low applied magnetic fields (<0.05 T) were prepared by placing polycrystalline solids in Mössbauer cups covered with Teflon lids. For high-field measurements, the solid materials were ground to finely divided powders and suspended in mineral oil. Samples of acetonitrile-wet crystals of **3** or **4** suspended in acetonitrile were placed in a Mössbauer cup and immediately frozen for experiments between 4.2 and 220 K. A sample of acetonitrile-wet crystals of **4** was prepared in a similar fashion except that all manipulations were done in a nitrogen-containing glovebox to prevent any exposure to oxygen. Spectral simulations were generated using WMOSS (WEB Research, Edina, MN), and isomer shifts are reported relative to Fe metal foil at room temperature.

X-ray Crystallography. Single-Crystal X-ray Diffraction. In a typical experiment, the crystal selected for study was suspended in polybutene oil (Aldrich), mounted on a cryoloop, and placed in an N_2 cold stream. In the low-temperature experiment at 30(1) K, a single crystal of **4** was mounted on a glass fiber attached to a rigid brass pin and cooled in a stream of He. Single crystals of compounds **1**−**5** rapidly lose interstitial solvent at room temperature and disintegrate when removed from the mother liquor. Therefore, in a room-temperature experiment, a crystal was drawn into a capillary and covered with mother liquor. The capillary was sealed on both ends with epoxy cement in such a way that the crystal was made to adhere to one of the ends. Single-crystal X-ray data were collected on a Bruker APEX or Bruker SMART 1000 diffractometer equipped with a CCD detector. The data sets were recorded as three ω-scans of 606 frames each, at 0.3° step width, and integrated with the Bruker SAINT software package.[31] The absorption correction (SADABS[32]) was based on fitting a function to the empirical transmission surface as sampled by multiple equivalent measurements. Solution and refinement of the crystal structures was carried out using the SHELX suite of programs[33] and the graphical interface X-SEED.[34] Preliminary indexing of the data sets established monoclinic unit cells for **1**−**4** and a trigonal unit cell for **5**. Systematic extinctions indicated that compounds **1**−**4** belong to the space group $P2_1/c$ (No. 14). Space group assignment for **5** was ambiguous as chiral space groups $P3_1$ (No. 144), $P3_2$ (No. 145), $P3_121$ (No. 152), and $P3_2$-21 (No. 154) were possible choices (vide infra). The structures were solved by direct methods, which resolved the positions of all metal atoms and most of the C and N atoms. The remaining non-hydrogen atoms were located by alternating cycles of least-squares refinements and difference Fourier maps. All hydrogen atoms were placed in calculated positions. All of the structures contain a large number of interstitial solvent molecules most of which were heavily disordered and could not be satisfactorily refined to a reasonable disorder model. Given the fact that the refinement of the basic structural unit, the TBP cluster, and especially the coordination geometries of metal ions are essentially uninfluenced by the presence of the disordered solvent, the SQUEEZE routine[35] was applied to subtract the diffraction contribution from the latter and to evaluate the number of solvent molecules present in the interstices. The final refinement was carried out with anisotropic thermal parameters for all non-hydrogen atoms. A summary of pertinent information relating to unit cell parameters, data collection, and refinement statistics is provided in Tables 1 and 2. Complete listings of positional and thermal parameters, bond distances, and bond angles as well as ORTEP plots of the asymmetric units (Figures S10−S14) are available as Supporting Information.

Additional Comments on the Crystallographic Refinement of 5. The crystal structure of **5** was solved in the chiral space group $P3_2$. After the non-disordered part of the structure was established and refined isotropically, the space group assignment was checked with PLATON,[35] which revealed additional symmetry elements. As a consequence, the symmetry was set to the space group $P3_221$. The refinement of the Flack parameter[36] indicated that the crystal was a racemic twin. An inversion twinning matrix was included in the final refinement, which revealed that the minor twin component contributed ∼13% of the observed diffraction intensities.

(29) Carlin, R. L. *Magnetochemistry*; Springer-Verlag: Berlin, Germany, 1986.
(30) Borrás-Almenar, J. J.; Clemente-Juan, J. M.; Coronado, E.; Tsukerblat, B. S. *J. Comput. Chem.* **2001**, *22*, 985−991.
(31) *SMART and SAINT*; Siemens Analytical X-ray Instruments Inc.: Madison, WI, 1996.
(32) Sheldrick, G. M. *SADABS*; University of Gottingen: Gottingen, Germany, 1996.
(33) Sheldrick, G. M. *SHELXS-97 and SHELXL-97*; University of Gottingen: Gottingen, Germany, 1997.
(34) Barbour, L. J. *J. Supramol. Chem.* **2001**, *1*, 189−191.
(35) Spek, A. L. *J. Appl. Crystallogr.* **2003**, *36*, 7−13.
(36) Flack, H. D. *Acta Crystallogr., Sect. A* **1983**, *A39*, 876−881.

Table 1. Crystal Data and Details of the Refinement Parameters for Compounds **1**, **2**, **3**, and **5**

formula	$Zn_3Cr_2N_{41}C_{142}H_{147}$ [**1**·17(CH_3CN)]	$Zn_3Fe_2N_{40}C_{140}H_{144}$ [**2**·16(CH_3CN)]	$Fe_5N_{38}C_{136}H_{138}$ [**3**·14(CH_3CN)]	$Fe_3Cr_2N_{46}C_{152}H_{162}$ [**5**·22(CH_3CN)]
space group	$P2_1/c$ (No. 14)	$P2_1/c$ (No. 14)	$P2_1/c$ (No. 14)	$P3_221$ (No. 154)
unit cell	a = 19.420(3) Å b = 25.613(4) Å c = 24.874(4) Å β = 97.498(3)°	a = 19.425(3) Å b = 25.331(4) Å c = 24.729(4) Å β = 98.142(3)°	a = 18.967(5) Å b = 24.818(7) Å c = 24.440(6) Å β = 97.682(6)°	a = 24.854(1) Å c = 20.228(2) Å γ = 120°
unit cell vol, V	12267(3) Å^3	12045(3) Å^3	11401(5) Å^3	10821(1) Å^3
Z	4	4	4	3
density, ρ_{calcd}	1.099 g/cm^3	1.124 g/cm^3	1.171 g/cm^3	0.922 g/cm^3
abs coeff, μ	0.799 mm^{-1}	0.874 mm^{-1}	0.674 mm^{-1}	0.482 mm^{-1}
cryst color and habit	colorless needle	yellow needle	burgundy red block	burgundy red block
cryst size	0.97 × 0.07 × 0.06 mm^3	0.80 × 0.06 × 0.06 mm^3	0.31 × 0.18 × 0.10 mm^3	0.24 × 0.12 × 0.05 mm^3
temp	150 K	150 K	110 K	150 K
radiation, λ	Mo Kα, 0.71073 Å	Mo Kα, 0.71073 Å	Mo Kα, 0.71073 Å	Mo Kα, 0.71073 Å
min and max, θ	1.15 to 23.26°	1.06 to 23.26°	1.17 to 28.43°	0.95 to 26.37°
reflns collected	75346 [R_{int} = 0.1471]	74253 [R_{int} = 0.1438]	117450 [R_{int} = 0.1358]	87889 [R_{int} = 0.0920]
independent reflns	17615	17320	26681	14746
data/parameters/restraints	17615/1258/0	17320/1258/0	26681/1259/0	14746/631/0
R [$F_o > 4\sigma(F_o)$]	R_1 = 0.0630 wR_2 = 0.1312	R_1 = 0.0727 wR_2 = 0.1582	R_1 = 0.0877 wR_2 = 0.1870	R_1 = 0.0818 wR_2 = 0.2061
GOF on F^2	1.000	1.072	0.981	1.008
max and min residual densities, e•Å^{-3}	0.430, −0.575	0.520, −0.450	0.623, −0.776	0.559, −0.434

Table 2. Crystal Data and Details of the Refinement Parameters for Compound **4**

formula	$Fe_3Co_2N_{31.7}C_{123.4}H_{119.1}$ [**4**·7.7(CH_3CN)]	$Fe_3Co_2N_{42}C_{144}H_{150}$ [**4**·18(CH_3CN)]	$Fe_3Co_2N_{35}C_{130}H_{129}$ [**4**·11(CH_3CN)]	$Fe_3Co_2N_{31.6}C_{123.2}H_{116.8}$ [**4**·7.6(CH_3CN)]
space group	$P2_1/c$ (No. 14)	$P2_1/c$ (No. 14)	$P2_1/c$ (No. 14)	$P2_1/c$ (No. 14)
unit cell	a = 19.113(4) Å b = 24.925(4) Å c = 24.674(5) Å β = 98.108(5)°	a = 19.159(4) Å b = 24.952(5) Å c = 24.709(5) Å β = 97.938(4)°	a = 19.24(2) Å b = 25.10(3) Å c = 24.89(3) Å β = 98.11(3)°	a = 19.49(1) Å b = 25.33(2) Å c = 25.15(2) Å β = 97.26(1)°
unit cell vol, V	11637(4) Å^3	11699(4) Å^3	11900(20) Å^3	12309(16) Å^3
Z	4	4	4	4
density, ρ_{calcd}	1.150 g/cm^3	1.144 g/cm^3	1.125 g/cm^3	1.088 g/cm^3
abs coeff, μ	0.697 mm^{-1}	0.693 mm^{-1}	0.681 mm^{-1}	0.658 mm^{-1}
cryst color and habit	burgundy red block	burgundy red block	burgundy red block	burgundy red block
cryst size	0.31 × 0.13 × 0.11 mm^3	0.45 × 0.22 × 0.08 mm^3	0.45 × 0.22 × 0.12 mm^3	0.47 × 0.33 × 0.15 mm^3
temp	30 K	110 K	200 K	298 K
radiation, λ	Mo Kα, 0.71073 Å	Mo Kα, 0.71073 Å	Mo Kα, 0.71073 Å	Mo Kα, 0.71073 Å
min and max, θ	1.08 to 23.26°	1.17 to 23.26°	1.07 to 28.49°	1.61 to 23.47°
reflns collected	21869 [R_{int} = 0.0630]	76232 [R_{int} = 0.1639]	98257 [R_{int} = 0.1311]	47425 [R_{int} = 0.2009]
independent reflns	14754	16757	28940	17339
data/parameters/restraints	14754/1234/48	16757/1259/0	28940/1259/0	17339/1198/0
R [$F_o > 4\sigma(F_o)$]	R_1 = 0.1019 wR_2 = 0.2354	R_1 = 0.0798 wR_2 = 0.1758	R_1 = 0.0826 wR_2 = 0.1721	R_1 = 0.0933 wR_2 = 0.2187
GOF on F^2	0.889	1.003	0.988	0.685
max and min residual densities, eÅ^{-3}	0.721, −0.893	0.648, −0.782	0.860, −1.312	0.796, −0.404

X-ray Powder Diffraction. Data were collected on Bruker Advance diffractometer equipped with monochromated Cu Kα radiation (λ = 1.54096 Å) in the 2θ range of 5−55°, with a step width of 0.02° at 2.5 s per data point.

Results

Synthesis. Reactions between divergent hexacyanometalate anions, $[M'^{III}(CN)_6]^{3-}$ (M′ = Cr, Fe, Co), and convergent mononuclear precursors of the type $[M^{II}(tmphen)_2X_2]^{0/2+}$ (M = Zn, Fe; X = Cl, CH_3CN) produce pentanuclear, cyanide-bridged complexes $[M^{II}(tmphen)_2]_3[M'^{III}(CN)_6]_2$ (Scheme 2). The synthesis is highly reproducible and can be easily scaled up. Compounds **1** and **2** were prepared in air and are air stable for an indefinite time. Compounds **3**−**5** were prepared under nitrogen but they are stable in solid form in air for an indefinite time.

TGA analyses were performed to determine the number of interstitial solvent molecules in water-containing samples of **1**−**5** and the thermal stability of the complexes (Figure S1). Gradual solvent loss occurred when the compounds were heated from room temperature to ∼120 °C. No solvent loss occurred after 120 °C and the compounds decomposed at ∼250 °C. The solvent content determined by this method varied between 7.5 and 10.5% by mass, depending on the compound. This mass difference corresponds to 8−13 molecules of water per molecule of complex, which is in agreement with the result of elemental analysis. Thus, thermogravimetric and elemental analyses support the conclusion that interstitial acetonitrile molecules are replaced with water molecules when compounds **1**−**5** are stored in air.

Molecular Structure Based on Low-Temperature X-ray Crystallography. Single-crystal X-ray studies revealed that **1**−**4** are isostructural and crystallize in the monoclinic space group $P2_1/c$. Compound **5** exhibits higher symmetry and crystallizes in the trigonal space group $P3_221$. The basic structural unit in

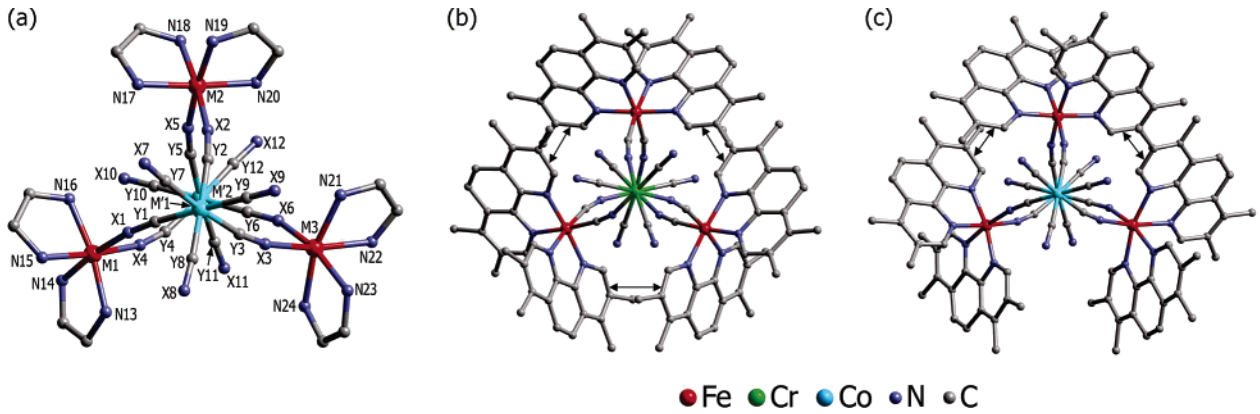

Figure 1. (a) Trigonal bipyramidal cluster $[M(tmphen)_2]_3[M'(CN)_6]_2$ viewed approximately along the axis of the bipyramid and showing the general atom labeling scheme for compounds **1**−**5**. For the sake of clarity, only four atoms of each tmphen ligand are shown; X, Y = C, N. (b, c) The TBP clusters in the structures of **5** and **4** in panels b and c, respectively. Intramolecular $\pi-\pi$ contacts are shown with black arrows. H atoms are omitted for the sake of clarity.

Scheme 2. Schematic Diagram of the Metal Ions in the TBP Cluster Core of Compounds **1**−**5**

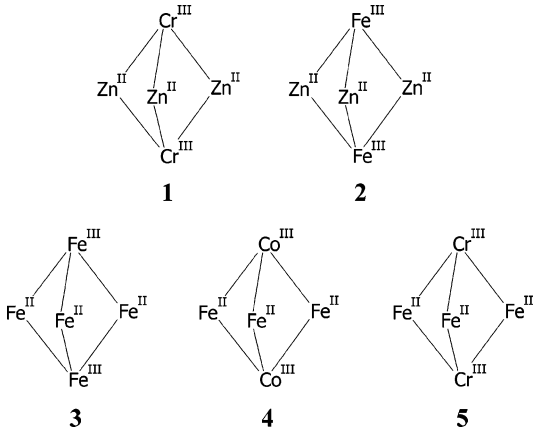

all compounds consists of a pentanuclear cluster with a trigonal bipyramidal, cyanide-bridged $M_3M'_2$ core (Figure 1a). Two hexacyanometalate anions $[M'(CN)_6]^{3-}$ occupy the axial positions of the core. Three cyanide ligands of each hexacyanometalate unit act as bridges, whereas the other three point away from the cluster. The three equatorial metal ions have pseudo-octahedral coordination, with two tmphen ligands acting as bidentate ligands and two CN^- ligands bridging the M and M′ ions.

The tmphen ligands are involved in intra- and intermolecular $\pi-\pi$ interactions. In the TBP cluster of **5**, each tmphen ligand is engaged in an intramolecular $\pi-\pi$ contact with a tmphen ligand from the neighboring Fe^{II} center (Figure 1b). The cluster resides on a 2-fold symmetry axis that passes through the Fe(2) center and bisects the Fe(1)−Fe(2)−Fe(3) angle. Therefore, two of the observed $\pi-\pi$ contacts are crystallographically equivalent (interplanar distance ∼3.6 Å), while the other $\pi-\pi$ distance is slightly longer (∼3.7 Å). Nevertheless, the equatorial triangle of Fe^{II} ions appears to be almost uniformly "wrapped" into a sheath of tmphen molecules. In contrast, the TBP clusters in **1**−**4** are less symmetric, with the three equatorial metal ions being nonequivalent and one of the intramolecular $\pi-\pi$ contacts being completely absent (Figure 1c). As a consequence, the interactions observed for tmphen ligands coordinated to the M(2) center are notably different from those exhibited by the tmphen ligands bound to M(1) and M(3).

Each pentanuclear TBP molecule consists of three equatorial metal centers of the same Δ or Λ chirality. The unit cell of **1**−**4** contains equal numbers of ΔΔΔ and ΛΛΛ molecules, which results in a low symmetry, centrosymmetric space group. In contrast, the unit cell of **5** contains clusters of the same chirality, which leads to a highly symmetric, enantiomorphic space group, but the crystals of **5** are racemically twinned.

Mass Spectrometry. Compounds **1** and **2** are insoluble in common solvents and thus could not be characterized by mass spectrometry. Compounds **3**−**5** are sparingly soluble in acetonitrile and slightly more soluble in 1:1 v/v acetonitrile−methanol. ESI mass spectrometry for **3**−**5** showed some fragmentation of the clusters under the conditions of electrospray ionization, which led to the mononuclear fragments $[Fe(tmphen)_2]^{2+}$ (m/z = 264) and $[Fe(tmphen)_3]^{2+}$ (m/z = 382). Intact clusters have been also observed in the mass spectrograms, as evidenced by the peaks located at m/z = 1269 [**3** + $Fe(tmphen)_2]^{2+}$, 1272 [**4** + $Fe(tmphen)_2]^{2+}$, 1387 [**3** + $Fe(tmphen)_3]^{2+}$, 1390 [**4** + $Fe(tmphen)_3]^{2+}$, and 1383 [**5** + $Fe(tmphen)_3]^{2+}$ (Figure S2). The charge of these fragments indicates that the clusters **3**−**5** are not oxidized in solution.

^{57}Fe Mössbauer Spectroscopy. Complexes **2**, **4**, and **5** have cores that contain Fe and another metal ion. We have used variable temperature, variable field ^{57}Fe Mössbauer spectroscopy to obtain direct information about the Fe ions present in the clusters.

In the case of complex **2**, which has a $[Zn^{II}_3Fe^{III}_2]$ core, there is no ambiguity about the oxidation state of Fe centers, which must be +3. The 50-K Mössbauer spectrum of **2** confirms this oxidation state as it consists of a quadrupole doublet with parameters indicative of LS Fe^{III} (Figure S3 and Table 3). The spectrum collected for the same sample at 4.2 K in a 0.05 T applied magnetic field is broad (not shown), which is indicative of the paramagnetism of the Fe sites.

X-ray crystallography indicates that compound **5** has an $[Fe_3Cr_2]^{12+}$ core. On the basis of the knowledge of redox properties of Fe and Cr ions, the most reasonable hypothesis for the oxidation states of the metal ions in the core of this compound is $[Fe^{II}_3Cr^{III}_2]$. At 4.2 K and room temperature in a low applied field, the compound exhibits a Mössbauer spectrum that consists of a sharp quadrupole doublet (Figure S4a). The lack of magnetic splitting in the 4.2 K spectrum suggests that diamagnetic or integer spin Fe sites are present in the cluster. The

Table 3. Mössbauer Parameters for the Fe Ions in Samples of **2**−**5**

compound		*T* (K)	δ *(mm/s)*	ΔE_Q (mm/s)	%[a]	Fe type
2		300	−0.13	0.55	100	Fe^{III}_{LS}
[Zn-Fe]		50	−0.05	0.94	100	Fe^{III}_{LS}
3	water-containing	300	0.36	0.27	40	Fe^{II}_{LS}
[Fe-Fe]	crystals		0.98	2.06	22	Fe^{II}_{HS}
			−0.14	0.7	39	Fe^{III}_{LS}
		220	0.38	0.4	54	Fe^{II}_{LS}
			0.99	2.56	8	Fe^{II}_{HS}
			−0.11	0.82	38	Fe^{III}_{LS}
		50	0.43	0.44	56	Fe^{II}_{LS}
			1.11	2.91	3	Fe^{II}_{HS}
			−0.04	0.96	41	Fe^{III}_{LS}
		4.2	0.44	0.44	60	Fe^{II}_{LS}
					<3[b]	Fe^{II}_{HS}
				broad		Fe^{III}_{LS}
3	acetonitrile-wet	220	0.39	0.40	41	Fe^{II}_{LS}
[Fe-Fe]	crystals		0.90	2.9	22	Fe^{II}_{HS}
			−0.01	0.90	37	Fe^{III}_{LS}
		4.2	0.44	0.47	55	Fe^{II}_{LS}
			1.16	2.9	3	Fe^{II}_{HS}
			−0.02	0.9	42	Fe^{III}_{LS}
4	water-containing	300	0.38	0.37	33	Fe^{II}_{LS}
[Fe-Co]	crystals		0.99	2.30	66	Fe^{II}_{HS}
		220	0.41	0.44	69	Fe^{II}_{LS}
			1.04	2.60	31	Fe^{II}_{HS}
		4.2	0.45	0.46	90	Fe^{II}_{LS}
			1.12	2.85	10	Fe^{II}_{HS}
4	acetonitrile-wet	220	0.41	0.46	47	Fe^{II}_{LS}
[Fe-Co]	crystals		1.05	2.75	53	Fe^{II}_{HS}
		4.2	0.45	0.46	80	Fe^{II}_{LS}
			1.12	2.99	20	Fe^{II}_{HS}
5		300	0.25	0.53	100	Fe^{II}_{LS}
[Fe-Cr]		4.2	0.33	0.58	100	Fe^{II}_{LS}

[a] Precision is ±2% of the value quoted. [b] Only an upper limit can be determined due to the broad feature assigned to LS Fe^{III}.

isomer shift and quadrupole splitting determined by simulation of the spectra (Table 3) are indicative of LS Fe^{II} ions. Spectra collected at the same temperature in an applied magnetic field of 8 T confirmed the diamagnetism of the Fe sites (Figure 2B). This result indicates unambiguously that at 4.2 K the cluster core of **5** is $[(LS\text{-}Fe^{II})_3Cr^{III}_2]$.

Clusters **3** and **4** have $[Fe_3Fe_2]^{12+}$ and $[Fe_3Co_2]^{12+}$ cores, respectively, and as +2 and +3 oxidation states are common for both Fe and Co, the assignment of these states to the three equatorial and two axial metal ions must be done carefully. At 4.2 K, the Mössbauer spectrum of a sample made of acetonitrile-wet crystals of **3** (Figures 3A and S6A) exhibits a doublet characteristic of LS Fe^{II} ($\delta/\Delta E_Q$ = 0.44/0.47 mm/s, Table 3) and one with Mössbauer parameters identical to those measured for the LS Fe^{III} sites in **2**, which accounted for 55% and 42% of the Fe in the sample, respectively. The 4.2-K Mössbauer spectrum of water-containing crystals of **3** showed a similar doublet for LS Fe^{II} representing ~60% of Fe in the sample, and a broad spectral feature indicative of paramagnetic Fe sites whose spin relaxation is intermediate (Figure 3b). This broad feature collapsed at 50 K into a quadrupole doublet (Figure 3A) similar to that observed at 4.2 K for the LS Fe^{III} in the sample of acetonitrile-wet crystals and accounting for 41% of the Fe in the sample. Therefore, at 4.2 K cluster **3** contains an $[(LS\ Fe^{II})_3Fe^{III}_2]$ core, and the interstitial solvent has no effect on

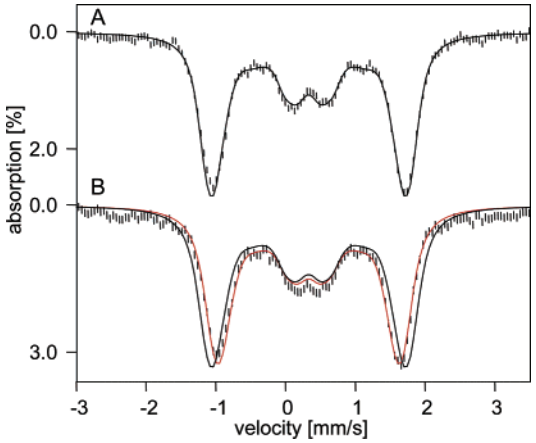

Figure 2. Mössbauer spectra of **5** recorded in a parallel external field of 8 T at 100 K (A) and 1.5 K (B). Simulations shown in black were obtained using a spin Hamiltonian containing nuclear hyperfine and nuclear Zeeman terms. The simulation drawn in red in panel B was obtained assuming an internal field of 0.6 T at the LS Fe^{II} nucleus.

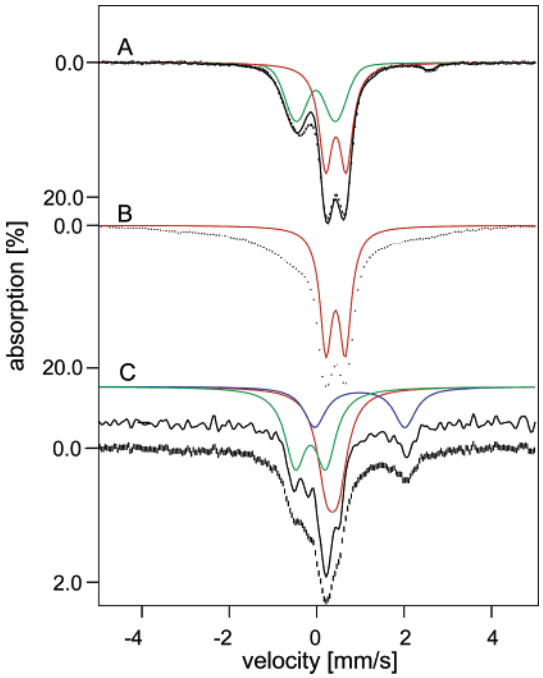

Figure 3. Selected 0.05-T Mössbauer spectra of **3**. (A) The 4.2-K spectrum of acetonitrile-wet crystals, with contributions from LS Fe^{II} and LS Fe^{III} shown in red and green, respectively. The black continuous line represents the 50-K spectrum recorded for the water-containing crystals. (B) The 4.2-K spectrum of water-containing crystals. The red line represents the contribution from LS Fe^{II}. (C) The 300-K spectrum of water-containing crystals. The red, blue, and green lines represent simulations of the contributions of LS Fe^{II}, HS Fe^{II}, and LS Fe^{III} ions, respectively. The black continuous line above the experimental data is a Fourier transform of the spectrum.

the electronic spin state of the metal ions in the cluster core and affects only the relaxation rate of the electronic spin.

Samples of acetonitrile-wet crystals of **3** have been studied up to 220 K, the temperature above which the acetonitrile that covered the crystals would melt, while samples of water-containing crystals have been studied up to room temperature. All samples contained at most 3% of HS Fe^{II} at 4.2 K. The amount of this species could be tracked between 4.2 and 50 K in samples of acetonitrile-wet crystals of **3** because the spin relaxation is fast and all types of Fe in the sample are represented by quadrupole doublets. Analysis of these spectra indicates that

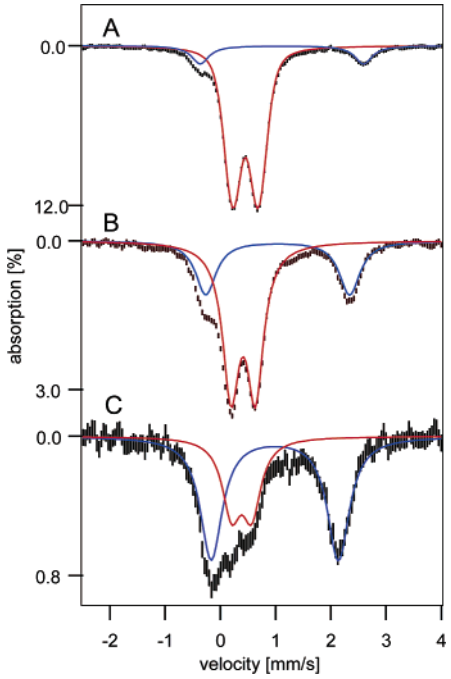

Figure 4. Mössbauer spectra for a water-containing sample of **4**, recorded at 4.2 (A) and 220 K (B) in 0.05 T applied magnetic field, and at 300 K (C). Contributions from LS and HS Fe^{II} ions are shown in red and blue, respectively.

the amount of HS Fe^{II} present at 4.2 K did not change up to 50 K (Figure S5a). Above 50 K, the amount of HS Fe^{II} increases with temperature. For example, comparison of the 50 and 100 K spectra for the acetonitrile-wet crystals shows clearly the increase in the absorption band at +2.1 mm/s, which is due to HS Fe^{II} (Figure S5b). Also, the 300 K Mössbauer spectrum of a sample of water-containing crystals of **3** shows an absorption band at +2.1 mm/s, which proves the existence in the sample of 20% HS Fe^{II} (blue line in Figure 3C), an amount significantly higher than that identified at 4.2 K, which was <3%. A Fourier transform procedure applied to this spectrum allowed us to remove the line-shape contribution of the Mössbauer source and to identify two absorption peaks on the left side of the spectrum (Figure 3C) that pertain to the LS Fe^{II} and LS Fe^{III} and represent 40% each of the total Fe in the sample (green and red lines in Figure 3C, respectively). The increase of the amount of HS Fe^{II} in the sample of water-containing crystals from 3% at 4.2−50 K to 8% at 220 K and 20% at room temperature is characteristic for a gradual LS Fe^{II} to HS Fe^{II} transition. The transition for acetonitrile-wet crystals of **3** starts at temperatures lower than that for water-containing crystals and leads to 22% of the Fe^{II} in the sample being HS at 220 K.

The 4.2 K, 0.05 T Mössbauer spectra for samples of both acetonitrile-wet and water-containing crystals of **4**, and for samples prepared in air or under nitrogen showed the presence of two types of Fe (Figure 4). The first type has Mössbauer parameters suggestive of LS Fe^{II} ($\delta/\Delta E_Q$ = 0.45/0.46 mm/s, Table 3) and represents 80−90% of Fe in the samples, and the second type has parameters characteristic of HS Fe^{II} ($\delta/\Delta E_Q \approx$ 1.1/2.9 mm/s, Table 3) and represents 10−20% of Fe in the samples. A 4.2-K, 8-T spectrum for water-containing crystals of **4** (Figure S6A), which had the maximum amount of the first type of Fe, showed that the majority of Fe is indeed diamagnetic, and thus LS Fe^{II}. The amount of HS Fe^{II} present in the samples at 4.2 K was variable, with 10−20% being encountered in the samples of acetonitrile-wet crystals and 10% being present in water-containing crystals. This HS Fe^{II} may represent an impurity or a population of clusters that contain HS Fe^{II} sites. We favor the latter assignment because powder diffraction studies of water-containing crystals of **4** show that the sample contains a unique crystalline phase, whose powder diffraction can be simulated using the unit cell parameters measured for single crystals of **4** in single-crystal X-ray diffraction measurements (Figure S7). Irrespective of the assignment of HS Fe^{II} as being part of the cluster or an impurity, Mössbauer spectroscopy determines unambiguously that the clusters in **4** have an $[Fe^{II}_3Co_2^{III}]$ core independent of the solvent content of the crystals.

A variable temperature Mössbauer study of **4** shows that increasing temperature leads to a major change in the cluster electronic structure (Figure 4). The amount of HS Fe^{II} present in any sample at 4.2 K did not change with the temperature up to 50 K (<20%), but at room temperature two-thirds of the Fe ions in the sample of water-containing crystals exhibit Mössbauer parameters characteristic of HS Fe^{II}, with the rest of the Fe ions remaining LS Fe^{II} (Table 3). This increase is most easily noted by the absorption band at +2.1 mm/s (Figure 4). A charge transfer induced spin transition similar to that observed for the related $[Co^{II}(tmphen)_2]_3[Fe^{III}(CN)_6]_2$ compound[18,19] is ruled out because the Fe oxidation state does not change with temperature. Instead, in the water-containing crystals of **4**, a "classical" spin transition occurs with increasing temperature at the equatorial $[Fe(tmphen)_2(NC)_2]$ sites, which either converts every TBP cluster from $[(LS\ Fe^{II})_3Co^{III}_2]$ at 4.2 K to $[(LS\ Fe^{II})(HS\ Fe^{II})_2Co^{III}_2]$ at room temperature or changes $^2/_3$ of the clusters in the sample from $[(LS\ Fe^{II})_3Co^{III}_2]$ to $[(HS\ Fe^{II})_3Co^{III}_2]$ over the same temperature interval. Variable temperature Mössbauer spectra for acetonitrile-wet crystals of **4** show that the spin transition also takes place in this material at even lower temperature than for the water-containing crystals (Figure S8 and Table 3).

The difference between the isomer shifts at 4.2 K of the LS Fe^{II} sites in the core of clusters **5** and **4**, that is, δ = 0.33 and 0.45 mm/s, respectively, is indicative of a difference in the CN^- coordination mode, with the lower value being characteristic of the coordination through the C-end of the ligand to create a $[Fe(tmphen)_2(\underline{C}N)_2]$ site and the higher value being indicative of the N-end coordination to create a $[Fe(tmphen)_2(\underline{N}C)_2]$ site.[37] The occurrence of the spin transition at the Fe^{II} sites in **4** but not in **5** further corroborates the hypothesis that they have $[Fe(tmphen)_2(NC)_2]$ and $[Fe(tmphen)_2(CN)_2]$ sites in the equatorial positions, respectively. The carbon-coordinated cyanide creates a stronger ligand field at the Fe sites as compared to the nitrogen-coordinated cyanide, thus making the Fe sites in **5** LS at all temperatures.

A careful examination of the 4.2-K, 8-T ^{57}Fe Mössbauer spectrum of cluster **5** (Figure 2B), which contains an $[Fe^{II}_2Cr^{III}_3]$ core, reveals the presence of Fe^{II} ions that are diamagnetic (S_{Fe} = 0), apart from the presence of a small internal field of 0.6 T at the Fe nucleus, which is antiparallel to the applied field (Figure 2B). We have verified, using a sample of potassium nitroprusside as a standard, that the applied magnetic field was indeed 8 T. Subsequently, we have collected Mössbauer spectra at this field and temperatures between 1.5 and 100 K (Figure 2). Interestingly, upon raising the temperature, the internal field

(37) Purcell, K. F.; Yeh, S. M.; Eck, J. S. *Inorg. Chem.* **1977**, *16*, 1708−1715.

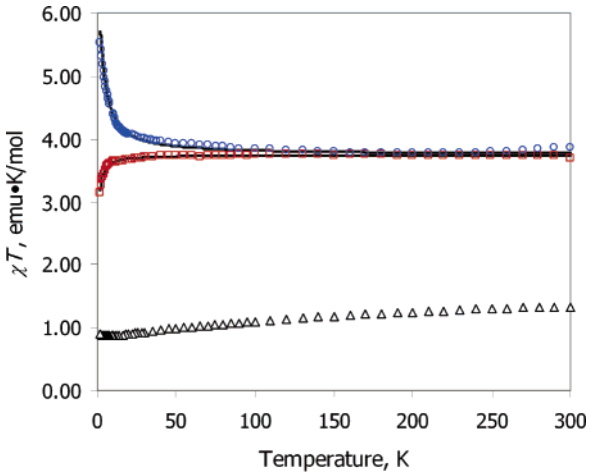

Figure 5. Temperature dependence of the χT product for compounds **1** (red squares), **2** (black triangles), and **5** (blue circles). The solid black lines correspond to the theoretical fits for **1** ($J_{Cr-Cr} = -0.08(1)$ cm^{-1}, $g_{Cr} = 2.00$, $R2 = 0.9995$) and **5** ($J_{Cr-Cr} = +0.65(5)$ cm^{-1}, $g_{Cr} = 2.00$, $R2 = 0.9964$). The correlation value is

$$R2 = 1 - \sqrt{\frac{\sum (\chi T_{obs} - \chi T_{calc})^2}{(n-p) \times \sum (\chi T_{obs})^2}}$$

where n is the number of experimental data points and p is the number of refined parameters.

at the iron nucleus decreases with the decreasing temperature in a manner similar to that of the magnetic susceptibility measured for the cluster (see below), which indicates that the 3d electrons of the diamagnetic Fe^{II} sites are spin polarized under the influence of the paramagnetic Cr^{III} ions (see below).

Magnetic Properties. Clusters **1** and **2** contain diamagnetic Zn^{II} ions in the equatorial positions, and therefore their magnetic properties are determined by the axial paramagnetic Cr^{III} and Fe^{III} ions, respectively. For compound **1**, which has a $[Zn_3Cr_2]$ core, the χT product is temperature independent above 10 K, and its high-temperature value agrees well with the spin-only value of 3.75 emu·K/mol expected for two Cr^{III} centers (Figure 5). The decrease in χT observed below 10 K can be attributed to weak antiferromagnetic coupling between the Cr^{III} ions mediated by the diamagnetic Zn^{II} centers[38] or to zero field splitting, which for the Cr^{III} ion is typically less than 1 cm^{-1}.[39] Assuming that only the former is in effect, the temperature dependence of χT can be modeled with the Heisenberg−Dirac−Van Vleck Hamiltonian $\hat{H} = -2J\hat{S}_{Cr(1)}\hat{S}_{Cr(2)}$, where J represents an isotropic magnetic exchange constant.[29] This results in a value of $J = -0.08$ cm^{-1} (Figure 5). If the same data is modeled assuming no exchange coupling and using a Hamiltonian that includes an axial zero field splitting at Cr^{III}, $\hat{H} = D[\hat{S}_z^2 - S(S+1)/3]$, a value of $D = 2.4$ cm^{-1} is obtained (Figure S9). This value is high for Cr^{III}, and therefore we favor the hypothesis of small exchange coupling between the axial Cr^{III} sites.[39] For compound **2**, which has a $[Zn_3Fe_2]$ core, the χT value of 1.33 emu·K/mol at room temperature is higher than the spin-only value of 0.75 emu·K/mol expected for two magnetically isolated LS Fe^{III} ions. Such a deviation has precedence for LS Fe^{III} complexes and is attributed to the strong orbital contribution and spin−orbit coupling.[40−42]

Complex **5**, $[Fe(tmphen)_2]_3[Cr(CN)_6]_2$, behaves as a paramagnet with a room temperature χT value corresponding to two isolated Cr^{III} centers (Figures 5 and 7).[5] This behavior suggests that the equatorial Fe^{II} ions are LS at all temperatures, which is in accord with the results of Mössbauer spectroscopy. The increase of χT at low temperatures is attributed to ferromagnetic coupling between the axial Cr^{III} ions mediated by the diamagnetic equatorial Fe^{II} ions,[6] because the action of zero field splitting (see Supporting Information, page 10) or antiferromagnetic coupling would lead to a decrease in χT. The temperature dependence of χT was modeled with the Heisenberg−Dirac−Van Vleck Hamiltonian, resulting in a value of $+0.65(5)$ cm^{-1} for the isotropic exchange coupling constant J (see later).

Compounds **3** and **4**, in which Fe^{II} ions reside in the equatorial positions of the TBP core and Fe^{III} or Co^{III} ions, respectively, occupy the axial positions, exhibit magnetic properties similar to each other. The magnetic properties of numerous samples of acetonitrile-wet and water-containing crystals of these compounds have been studied.

The χT value measured for water-containing crystals of **3** below 100 K (Figure 6a) reflects the contribution of the LS Fe^{III} sites in the $[Fe^{II}_3Fe^{III}_2]$ core and is comparable to that measured for **2**, which contains a $[Zn^{II}_3Fe^{III}_2]$ core. Therefore the three Fe^{II} sites of the cluster **3** must be LS up to 100 K, in agreement with the result of Mössbauer spectroscopy. The χT observed for the water-containing crystals of **4** below 100 K (∼0.8 emu/mol, Figure 6b) is assigned to paramagnetic HS Fe^{II}, which is in agreement with the result of Mössbauer spectroscopy. The diamagnetic Co^{III} ions in the axial positions have only a very small temperature-independent paramagnetic contribution estimated to be $\sim 3 \times 10^{-4}$ emu/mol.[29] The χT product for water-containing crystals of both **3** and **4** gradually increases by ∼9 emu·K/mol in the temperature range 100−375 K (Figure 6). When the LS Fe^{III} contribution is subtracted from the χT value of **3** at 300 K, a value of 5.3 emu·K/mol is obtained for the Fe^{II} centers, which corresponds to ∼1.8 HS Fe^{II} ions per $Fe^{II}_3Fe^{III}_2$ cluster. This is in agreement with the conclusion reached by Mössbauer spectroscopy. Therefore, the increase in χT is assigned to the LS to HS transition at the three Fe^{II} sites of the clusters. The χT product for samples of acetonitrile-wet crystals of **3** and **4** also increases with temperature, but the increase is more gradual and its onset is at lower temperature as compared to the water-containing samples (Figure 6). This finding is also in agreement with the observations made by Mössbauer spectroscopy.

X-ray Crystallography. The bond lengths in the $[Fe(CN)_6]^{n-}$ anions, which contain LS Fe^{II} or LS Fe^{III} ions, are not very sensitive to the Fe oxidation state. For example, a search of the current entries (August 2006; structures with $R < 0.052$) in the Cambridge Crystallographic Database shows that the Fe−C and C−N distances in $[Fe(CN)_6]^{3-}$ complexes are in the 1.859−1.994 and 1.103−1.163 Å range, respectively, while the corresponding intervals for $[Fe(CN)_6]^{4-}$ complexes are 1.882−1.935 and 1.138−1.191 Å, respectively. On the contrary, LS to HS spin transitions at Fe^{II} centers significantly affect the metal−ligand bond lengths and cause changes of their octahedral

(38) Journaux, Y.; Sletten, J.; Kahn, O. *Inorg. Chem.* **1986**, *25*, 439−447.
(39) Boca, R. *Coord. Chem. Rev.* **2004**, *248*, 757−815; Chirico, R. D.; Carlin, R. L. *Inorg. Chem.* **1980**, *19*, 3031−3033.
(40) Figgis, B. N. *Trans. Faraday Soc.* **1961**, *57*, 198−203.
(41) Figgis, B. N.; Gerloch, M.; Mason, R. *Proc. R. Soc. London, Ser. A* **1969**, *309*, 91−118.
(42) Baker, J.; Figgis, B. N. *Aust. J. Chem.* **1982**, *35*, 265−275.

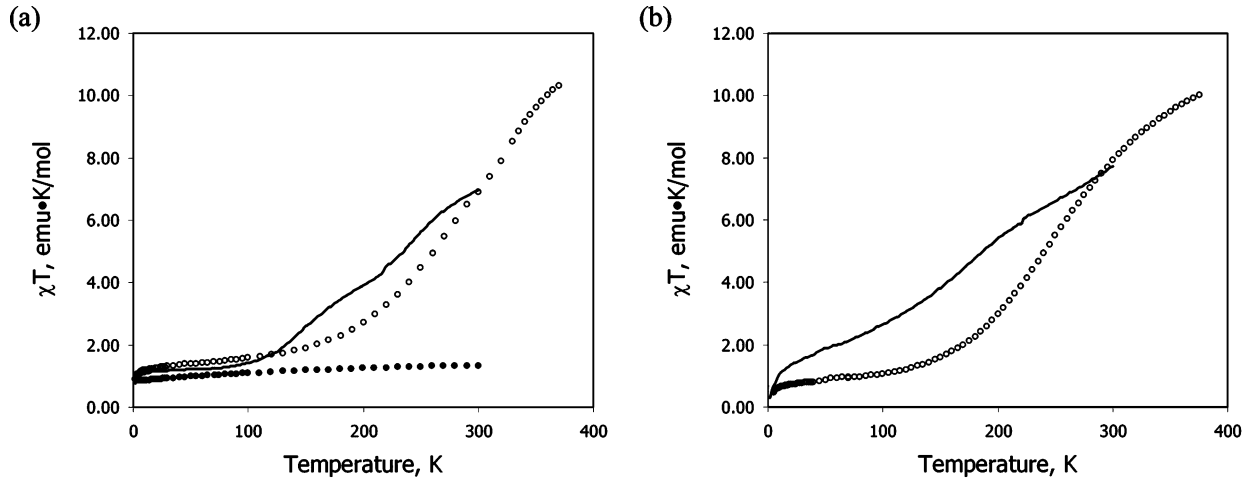

Figure 6. (a) Temperature dependence of the χT product for water-containing crystals of **3** (open circles) and for acetonitrile-wet crystals of **3** (solid line). For comparison, the behavior of χT for **2** is also shown (filled circles). (b) Temperature dependence of the χT product for water-containing crystals of **4** (open circles) and for acetonitrile-wet crystals of **4** (solid line).

Table 4. Metal−Ligand Bond Distances (Å) in the Crystal Structures of **1** (150 K), **2** (150 K), **3** (110 K), and **5** (150 K)[a]

	equatorial			axial	
compound	M1–X	M2–X	M3–X	M′1–Y	M′2–Y
1 (Zn−Cr) M = Zn; M′ = Cr; X = N; Y = C	*2.039(7)*	*2.092(7)*	*2.064(6)*	*2.037(8)*	*2.074(9)*
	2.068(7)	*2.093(7)*	*2.115(6)*	*2.052(8)*	*2.080(8)*
	2.168(6)	2.126(6)	2.138(6)	*2.100(9)*	*2.116(9)*
	2.172(6)	2.144(6)	2.153(6)	2.010(9)	2.043(9)
	2.180(6)	2.183(6)	2.176(6)	2.05(1)	2.058(8)
	2.181(6)	2.184(7)	2.218(6)	2.10(1)	2.065(9)
2 (Zn−Fe) M = Zn; M′ = Fe; X = N; Y = C	*2.056(7)*	*2.077(7)*	*2.053(7)*	*1.91(1)*	*1.935(9)*
	2.115(7)	*2.097(8)*	*2.080(7)*	*1.93(1)*	*1.94(1)*
	2.133(6)	2.128(7)	2.175(6)	*1.942(9)*	*1.97(1)*
	2.165(7)	2.173(7)	2.179(7)	1.942(9)	1.877(9)
	2.197(7)	2.179(8)	2.181(7)	1.96(1)	1.92(1)
	2.223(7)	2.202(7)	2.217(7)	1.97(1)	1.94(1)
3 (Fe−Fe) M = Fe; M′ = Fe; X = N; Y = C	*1.853(5)*	*1.923(5)*	*1.895(5)*	*1.874(8)*	*1.925(7)*
	1.943(6)	*1.939(6)*	*1.928(6)*	*1.913(7)*	*1.945(7)*
	1.910(5)	1.954(5)	1.943(6)	*1.952(7)*	*1.950(7)*
	1.961(4)	1.954(6)	1.947(5)	1.900(8)	1.900(7)
	1.966(5)	1.960(5)	1.966(5)	1.910(8)	1.909(8)
	1.986(5)	1.968(6)	1.968(5)	1.933(7)	1.931(8)
5 (Fe−Cr)[b] M = Fe; M′ = Cr; X = C/N; Y = N/C	*1.915(6)*	*1.910(4)*	*1.915(6)*	*2.049(5)*	*2.049(5)*
	1.925(5)	*1.910(4)*	*1.925(5)*	*2.059(6)*	*2.059(6)*
	1.949(6)	1.966(5)	1.949(6)	*2.103(6)*	*2.103(6)*
	1.959(5)	1.966(5)	1.959(5)	2.052(7)	2.052(7)
	1.979(6)	1.983(4)	1.979(6)	2.070(6)	2.070(6)
	1.979(6)	1.983(4)	1.979(6)	2.071(6)	2.071(6)

[a] Bonds to the cyanide ligands are in italic. [b] In the structure of **5**, the M1 and M3 centers are crystallographically equivalent, as are the M′1 and M′2 centers.

coordination geometry. The average Fe−N distances in LS and HS complexes of $[FeN_6]$ type are 1.92−2.00 and 2.16−2.21 Å, respectively.[43] The deformation of the octahedral geometry can be quantified by the change in the parameter Σ, defined as the sum of the deviations from 90° of the 12 cis N−Fe−N angles. While Σ is 0 for an ideal octahedron, for LS and HS $[FeN_6]$ complexes this parameter is ∼30 to 50° and ∼70 to 90°, respectively. To study these changes, the crystal structure of complex **4**, which undergoes a spin transition, was determined at several temperatures between 30 and 298 K (Table 5), and the structural parameters for the cluster at these temperatures

Table 5. Metal−Ligand Bond Distances (Å) and Parameter Σ (deg) in the Crystal Structure of **4** at Different Temperatures (M = Fe; M′ = Co; X = N; Y = C)[a]

	equatorial			axial	
temperature	M1–X	M2–X	M3–X	M′1–Y	M′2–Y
30 K	*2.026(3)*	*1.924(3)*	*1.946(4)*	*1.852(4)*	*1.870(3)*
	2.084(3)	*1.927(4)*	*1.958(3)*	*1.891(4)*	*1.917(4)*
	2.115(4)	1.917(3)	1.936(3)	*1.895(4)*	*1.925(5)*
	2.133(3)	1.929(3)	1.943(3)	1.814(5)	1.886(5)
	2.139(3)	1.955(3)	1.961(3)	1.836(5)	1.890(3)
	2.187(4)	1.992(4)	1.985(4)	1.909(4)	1.909(4)
average M−L	2.11	1.94	1.95	1.87	1.90
Σ	72.2	39.8	41.3		
110 K	*2.024(2)*	*1.944(2)*	*1.945(2)*	*1.880(3)*	*1.859(3)*
	2.054(3)	*1.956(2)*	*1.961(2)*	*1.897(3)*	*1.872(3)*
	2.080(3)	1.954(2)	1.948(3)	*1.925(3)*	*1.892(3)*
	2.093(3)	1.961(2)	1.960(2)	1.831(3)	1.823(3)
	2.100(3)	1.962(2)	1.963(2)	1.887(3)	1.869(3)
	2.129(3)	1.977(2)	1.971(2)	1.921(3)	1.900(3)
average M−L	2.08	1.96	1.96	1.87	1.87
Σ	71.8	40.6	43.9		
200 K	*2.070(4)*	*1.938(5)*	*1.972(5)*	*1.881(6)*	*1.861(5)*
	2.106(6)	*1.939(5)*	*2.002(6)*	*1.884(7)*	*1.885(7)*
	2.168(5)	1.955(5)	1.996(5)	*1.903(5)*	*1.885(7)*
	2.179(5)	1.958(5)	2.007(4)	1.853(7)	1.858(7)
	2.184(5)	1.976(5)	2.007(5)	1.879(8)	1.890(7)
	2.200(5)	1.976(5)	2.012(5)	1.901(6)	1.902(5)
average M−L	2.15	1.96	2.00	1.90	1.88
Σ	77.1	40.6	52		
298 K	*2.120(6)*	*1.954(7)*	*2.087(7)*	*1.821(9)*	*1.824(8)*
	2.123(6)	*1.989(8)*	*2.116(7)*	*1.899(8)*	*1.854(8)*
	2.181(7)	1.954(7)	2.138(6)	*1.918(9)*	*1.864(9)*
	2.196(7)	1.959(7)	2.160(7)	1.86(1)	1.799(8)
	2.201(6)	1.979(8)	2.194(7)	1.893(9)	1.82(1)
	2.225(7)	1.998(6)	2.233(6)	1.920(9)	1.88(1)
average M−L	2.17	1.97	2.15	1.89	1.84
Σ	78.5	45.5	80.0		

[a] Bonds to the cyanide ligands are in italic.

were compared to those measured for the Fe sites in complexes **2**, **3**, and **5** at 110−150 K (Table 4).

Complexes **2** and **5** contain $[Fe^{III}(CN)_6]$ and $[Fe^{II}(tmphen)_2(CN)_2]$ sites, respectively (Figure 1). The Fe^{III}−CN distances observed in the 150 K crystal structure of **2**, namely 1.91(1)−1.960(9) Å for the terminal cyanides and 1.876(9)−1.97(1) Å for the bridging cyanides, are comparable to the Fe−CN bond lengths of 1.929(5)−1.944(8) Å in $K_3[Fe(CN)_6]$.[44] The Fe^{II}−N_{tmphen} and Fe^{II}−$C_{cyanide}$ bond lengths in the 150 K crystal

(43) Guionneau, P.; Marchivie, M.; Bravic, G.; Létard, J. F.; Chasseau, D. *Top. Curr. Chem.* **2004**, *234*, 97−128.

Table 6. C≡N Stretching Frequencies in Complexes **1**−**5**, Corresponding PB Analogues, and Free Hexacyanometalate Anions[a]

	ν(C≡N), cm^{-1}			
compound	bridging	terminal	PB analogue	free $[M'(CN)_6]^{3-}$ [b]
1 ($Zn^{II}_3Cr^{III}_2$)	2172, 2162, 2152	2125	2165[53]	2114
2 ($Zn^{II}_3Fe^{III}_2$)	2165, 2156, 2142	2117, 2112	2175[50]	2101
3 ($Fe^{II}_3Fe^{III}_2$)	2131	2109	not reported[c]	2101
4 ($Fe^{II}_3Co^{III}_2$)	2167, 2156, 2147	2127	2165[50]	2126
5 ($Fe^{II}_3Cr^{III}_2$)	2103	2117	2162 or 2098[51]	2114

[a] Both complexes **1**−**5** and their PB type counterparts contain varying amounts of interstitial solvent. The influence of these solvent molecules on the ν(C≡N) values is insignificant. [b] The ν(C≡N) stretches of free $[M'(CN)_6]^{3-}$ anions were measured for $(TEA)_3[Cr(CN)_6]$, $(TMA)_3[Fe(CN)_6]$, and $[(18\text{-crown-6})K]_3[Co(CN)_6]$ (TEA = tetraethylammonium, TMA = tetramethylammonium). [c] See discussion.

structure of **5** are close to the corresponding values for the LS mononuclear complex $[Fe(phen)_2(CN)_2]$, which are 1.966−2.007 and 1.856−1.917 Å, respectively.[45,46]

At 110 K, the average Fe^{II}−N distances for the three equatorial $[Fe(tmphen)_2(NC)_2]$ units in the structure of **3** are 1.94, 1.95, and 1.95 Å, which are typical for LS Fe^{II} in this type of coordination environment.[43] The $\sum$ parameters for the three Fe sites are between 38° and 44° and are also indicative of LS Fe^{II}. The range of the $Fe^{II}-N_{tmphen}$ bond lengths in the cluster (1.920(5)−1.988(5) Å) is comparable to those observed for the LS forms of the $[Fe(phen)_2(NCX)_2]$ complexes (X = S, Se),[47,48] which are 1.990(3)−2.007(2) and 1.971(2)−1.997(2) Å, respectively. Five out of six $Fe^{II}-N_{cyanide}$ distances are comparable to the Fe−NCX distances measured in $[Fe(phen)_2(NCX)_2]$. One of the $Fe^{II}-N_{cyanide}$ bonds is significantly shorter (1.857(5) Å) but is similar to the Fe^{II}−N distance of 1.87(1) Å reported for *trans*-$[Fe^{II}(NCMe)_2(dppm)_2][Fe^{II}I_4]\cdot 2H_2O$ (dppm = bis(diphenylphosphino)methane).[49]

At 30 and 110 K, the average bond lengths and $\sum$ for the equatorial Fe(2) and Fe(3) ions in complex **4** are characteristic of LS Fe^{II} (Table 5). The corresponding parameters for Fe(1) are significantly higher than for the other two Fe sites suggesting significant HS Fe^{II} character, although they are lower than the values typically reported for HS Fe^{II} sites. Typically the bond lengths determined for a compound by X-ray crystallography at multiple temperatures show a small decrease with the increasing temperature due to an increase in the amplitude of the atom vibrations. This is the case above 110 K for the average Co−N bond lengths in **4** but not for the Fe−N bonds, which show a systematic increase. At room temperature, both the Fe−N bond lengths and $\sum$ for Fe(1) and Fe(3) are typical of HS Fe^{II}. These parameters also increase for Fe(2) but only to a small extent. The temperature-induced changes in the cluster geometry indicate that a spin transition occurs at the Fe^{II} sites. For Fe(2), the transition is not complete at room temperature, which is the highest temperature at which we have collected Mössbauer spectra and single-crystal diffraction data. Close examination of the crystal structure of **4** shows that the Fe(2) center is different from the other equatorial sites, Fe(1) and Fe(3), as both of its tmphen ligands engage in intramolecular $\pi-\pi$ interactions with the tmphen ligands on the Fe(1) and Fe(3) centers (see earlier).

Infrared Spectroscopy. IR spectra of complexes **1**−**5** in the region of the C≡N stretching frequencies provide information about the metal ion oxidation state and the cyanide ligand binding mode. The energy of the ν(C≡N) stretch increases with the metal oxidation state and is also higher when the cyanide acts as a bridging ligand.[16] For example, the ν(C≡N) modes of $K_4[Fe(CN)_6]$ and $K_3[Fe(CN)_6]$ are in the ranges of 2020−2030 and 2115−2125 cm^{-1}, respectively, and those of $M^{II}-CN-M'^{III}$ are found at 2100−2165 cm^{-1}.[50] Complexes **1**−**5** contain terminal cyanide ligands coordinated to M^{III} ions and bridging cyanides that can be of either $M^{II}-N\equiv C-M'^{III}$ or $M^{II}-C\equiv N-M'^{III}$ type. Studies of $Fe^{II}-Cr^{III}$ analogues of Prussian blue have shown that the two bridging modes can be distinguished based on the IR frequencies, with the former mode exhibiting higher cyanide stretching frequencies than the latter.[51,52] A similar trend has been noted for the $Fe^{II}-C\equiv N-BH_3$ and $Fe^{II}-N\equiv C-BH_3$ bridging modes in $[Fe(phen)_2(CNBH_3)_2]$ and $[Fe(phen)_2(NCBH_3)_2]$, respectively.[37]

Complexes **1**−**5** exhibit several ν(C≡N) stretches at lower frequencies that are in the same range as those found for free hexacyanometalate anions (Table 6); consequently, we attribute these IR modes to the terminal CN^- ligands. Complexes **1**−**4** also display ν(C≡N) stretches that are shifted by ∼20 to 50 cm^{-1} to higher energies than the bands of free $[M'(CN)_6]^{3-}$ anions. A comparison with the IR spectra of Prussian blue analogues supports the assignment of these bands to the $M^{II}-N\equiv C-M'^{III}$ bridging mode.[51,52] On the contrary, compound **5** displays a lower frequency feature at 2103 cm^{-1}, which is attributed to a $M^{II}-C\equiv N-M'^{III}$ bridging cyanide mode. This assignment, which is indicative of cyanide linkage isomerism in **5**, is in accord with the results of Mössbauer spectroscopy and magnetic studies.

Discussion

The reactions of hexacyanometalates that contain trivalent metal ions and mononuclear complexes of divalent metal ions coordinated to two tmphen ligands afford a series of homologous, heterometallic cyanide-bridged clusters. These clusters consist of a trigonal bipyramidal core of metal ions in which

(44) Figgis, B. N.; Skelton, B. W.; White, A. H. *Aus. J. Chem.* **1978**, *31*, 1195−1199.
(45) Zhan, Z.; Meng, Q.; You, X.; Wang, G.; Zheng, P. J. *Polyhedron* **1996**, *15*, 2655−2658.
(46) Harada, K.; Yuzurihara, J.; Ishii, Y.; Sato, N.; Kambayashi, H.; Fukuda, Y. *Chem. Lett.* **1995**, 887−888.
(47) Marchivie, M.; Guionneau, P.; Howard, J. A. K.; Chastanet, G.; Létard, J. F.; Goeta, A. E.; Chasseau, D. *J. Am. Chem. Soc.* **2002**, *124*, 194−195.
(48) MacLean, E. J.; McGrath, C. M.; O'Connor, C. J.; Sangregorio, C.; Seddon, J. M. W.; Sinn, E.; Sowrey, F. E.; Teat, S. J.; Terry, A. E.; Vaughan, G. B. M.; Young, N. A. *Chem.−Eur. J.* **2003**, *9*, 5314−5322.
(49) Barclay, J. E.; Evans, D. J.; Hughes, D. L.; Leigh, G. J. *J. Chem. Soc., Dalton Trans.* **1993**, 69−73.
(50) Fernández Bertrán, J.; Reguera-Ruíz, E.; Blanco Pascual, J. *Spectrochim. Acta, Part A* **1990**, *46A*, 1679−1682.
(51) Reguera, E.; Bertrán, J. F.; Nuñez, L. *Polyhedron* **1994**, *13*, 1619−1624.
(52) Coronado, E.; Gimenez-Lopez, M. C.; Levchenko, G.; Romero, F. M.; Garcia-Baonza, V.; Milner, A.; Paz-Pasternak, M. *J. Am. Chem. Soc.* **2005**, *127*, 4580−4581.
(53) Griebler, W. D.; Babel, D. *Z. Naturforsch., B: Chem Sci.* **1982**, *37B*, 832−837.

the two axial positions are occupied by $[M'(CN)_6]^{3-}$ ions and the three equatorial positions by $[M(tmphen)_2(CN)_2]$ units. Clusters **1**−**4** contain $M^{II}-N\equiv C-M'^{III}$ bridges, which indicates that the $M'^{III}-CN$ bonds present in the hexacyanometalate starting materials remain intact during cluster assembly. This cyanide bridging mode is different from the $Fe^{II}-C\equiv N-Fe^{III}$ one existent in Prussian blue irrespective of its synthesis either from Fe^{2+} and $[Fe(CN)_6]^{3-}$ or from Fe^{3+} and $[Fe(CN)_6]^{4-}$ precursors. Cluster **5** contains $M^{II}-C\equiv N-M'^{III}$ bridges, an indication that a cyanide flip takes place during its synthesis. This phenomenon had been previously documented for the $Fe^{II}-Cr^{III}$ analogue of Prussian blue.[51]

The coexistence of cyanide-bridged Fe^{II} and $[Fe^{III}(CN)_6]^{3-}$ ions in **3** is unprecedented in the PB family. The cluster is the closest molecule to the purported $Fe^{II}_3[Fe^{III}(CN)_6]_2$ (Turnbull blue), which was long considered to be different from the $Fe^{III}_4[Fe^{II}(CN)_6]_3$ (Prussian blue), until Robin conclusively showed in 1962 that they are the same compound corresponding to the latter formula.[2] Recently, a compound dubbed "Ukrainian red" has been reported as the first prototype of the elusive Turnbull blue,[54] but the compound contains a complex Fe^{II} cation that is isolated from the $[Fe^{III}(CN)_6]^{3-}$ counterion. In contrast, in the crystal structure of **3**, the $[Fe^{III}(CN)_6]^{3-}$ fragment is directly connected to Fe^{II} centers through CN^- bridges.

The $[FeN_6]$ coordination environment of the equatorial Fe^{II} ions in clusters **3** and **4** produces a ligand field for which thermally induced spin crossover is possible. The occurrence of such a transition was demonstrated by: (1) magnetic susceptibility, which probes the overall properties of the polynuclear compounds, showed an increase in the magnetic moment of the clusters; (2) Mössbauer spectroscopy, which provides information on each type of Fe ion in the clusters, demonstrated unequivocally that the amount of HS Fe^{II} ions in the clusters increases with the temperature at the expense of the amount of LS Fe^{II} in the samples; (3) X-ray crystallography, which showed changes of ∼0.20 Å in the Fe−N bond lengths with the temperature. The latter method established that changes in the spin state occurs at specific Fe sites in each cluster in the crystal and do not occur with intramolecular cooperativity, which would lead to $[(HS-Fe^{II})_3Co_2]$ cores.

The magnetic data of water-containing crystals of **3** reveal that the χT value at 300 K is 6.9 emu·K/mol. If the contribution of Fe^{III} to χT is the same as that measured for cluster **2** at the same temperature, and the TIP of the equatorial Fe^{II} ions is taken into account, one obtains a contribution of 5.2 emu·K/mol for the Fe^{II} centers. The magnetic moment of a HS Fe^{II} ion is affected by the orbital contribution, with the largest χT value of 3.9 emu·K/mol having been reported.[55] Assuming this value for χT, we determine that there would be 1.3 HS Fe^{II} ions/cluster, which is close to that determined from Mössbauer data, namely 1 HS Fe^{II} ion/cluster. Nevertheless, the estimate of $\chi T \approx 3.9$ emu·K/mol for the HS Fe^{II} ions in cluster **3** may be too large because the coordination of the Fe^{II} is similar to that of the pseudo-octahedral *cis*-$[Fe(phen)_2(NCS)_2]$ complex,[20] for which χT/Fe^{II} is only 3.4 emu·K/mol. If we adopt this smaller value of χT/HS Fe^{II}, we calculate that there would be 1.5 HS Fe^{II}/cluster at room temperature, which is 50% larger than the value determined by Mössbauer spectroscopy. A reason for the difference between the estimate for the number of HS Fe^{II} ions based on magnetic susceptibility and that based on Mössbauer spectroscopy may be differences in sample preparation and composition. Although the samples for Mössbauer and magnetic measurements were taken from the same synthetic batch, the solvent content is likely to be significantly different in these samples because samples are exposed to vacuum in the SQUID cavity while Mössbauer samples are not.

The crystal structure determination carried out at 30 and 110 K on single crystals of **4** revealed that one of the three equatorial Fe^{II} ions is different from the other two and has bond lengths characteristic of HS Fe^{II}. Low-temperature Mössbauer and magnetic susceptibility of acetonitrile-wet and water-containing crystals confirmed the presence of HS and LS Fe^{II} ions in the clusters and showed that the content of HS Fe^{II} is 10−20% in the former and ∼10% in the latter. These measurements indicate that the clusters have an $[Fe^{II}_3Co^{III}_2]$ core and that the spin state of the Fe^{II} ions is sensitive to the crystallization solvent, with acetonitrile favoring the HS over the LS state. Variable temperature magnetic measurements and Mössbauer spectroscopy studies have shown that, irrespective of the solvent, the LS to HS transition occurs at the Fe^{II} sites, and that in the case of acetonitrile-wet crystals, the transition starts at lower temperature and is less abrupt.

The spin transition observed at the Fe^{II} sites in both clusters is gradual, irrespective of the solvent present in the crystals of **3** and **4**, which is indicative of weak cooperativity and consequently weak intermolecular interactions between the molecules situated in the crystals of **3** and **4**. Indeed, we have observed weak intermolecular interactions of $\pi-\pi$ type mediated by the tmphen ligands. The lack of strong intermolecular interactions has been also evidenced in the isostructural compound $[Mn^{II}(tmphen)_2]_3[Mn^{III}(CN)_6]_2$, which exhibits single molecule magnetism.[17] As has been mentioned previously, the hypothetical Turnbull blue structure with Fe^{III} ions in the carbon-bound sites does not exist. We hypothesize, however, that if this $AFe^{II}[Fe^{III}(CN)_6]$ material could be isolated (where A is an alkali metal cation), it might exhibit a spin transition with enhanced cooperativity owing to the extended 3D structure of the material. Indeed, a recent report indicates that $CsFe^{II}[Cr^{III}(CN)_6]$ compound, in which most of the Fe^{II} sites are N-bound, has an abrupt spin transition with a 27 K thermal hysteresis loop.[56] This report, along with the observation of spin crossover in cluster **4** that has the $[Fe^{II}_3Co^{III}_2]$ core, hints at the potential to observe an abrupt spin transition in the $AFe^{II}[Co^{III}(CN)_6]$ solids. We currently pursue the preparation of such materials in our laboratories.

The characteristics of the spin transition of **3** and **4**, that is, abruptness and transition temperature, depend significantly on the amount and/or type of solvent present in the crystals. Such differences in solvent content have been shown to influence significantly the spin crossover behavior of Fe^{II} complexes.[57−59]

(54) Pavlishchuk, V. V.; Koval, I. A.; Goreshnik, E.; Addison, A. W.; Van Albada, G. A.; Reedijk, J. *Eur. J. Inorg. Chem.* **2001**, 297−301.
(55) Madeja, K.; König, E. *J. Inorg. Nucl. Chem.* **1963**, *25*, 377−385.
(56) Kosaka, W.; Nomura, K.; Hashimoto, K.; Ohkoshi, S. *J. Am. Chem. Soc.* **2005**, *127*, 8590−8591.
(57) Stassen, A. F.; De Vos, M.; van Koningsbruggen, P. J.; Renz, F.; Ensling, J.; Kooijman, H.; Spek, A. L.; Haasnoot, J. G.; Gütlich, P.; Reedijk, J. *Eur. J. Inorg. Chem.* **2000**, 2231−2237.
(58) Roubeau, O.; Haasnoot, J. G.; Codjovi, E.; Varret, F.; Reedijk, J. *Chem. Mater.* **2002**, *14*, 2559−2566.
(59) Bonhommeau, S.; Molnár, G.; Galet, A.; Zwick, A.; Real, J. A.; McGarvey, J. J.; Bousseksou, A. *Angew. Chem., Int. Ed.* **2005**, *44*, 4069−4073.

For example, the hydrated complex $\{Fe(pyrazine)[Pt(CN)_4]\}\cdot nH_2O$ ($n = 2,3$) undergoes a gradual transition centered at 230 K and in which χT changes by ~3 cm^3 K/mol, whereas the dehydrated complex ($n = 0$) exhibits a more abrupt spin crossover behavior centered at room temperature and in which χT changes by ~3.65 cm^3 K/mol.[59]

Exchange interactions between paramagnetic metal ions mediated by bridges that contain diamagnetic metal ions were realized decades ago for Prussian blue, which behaves as a ferromagnet with $T_C = 5.5$ K.[7] Ferromagnetic couplings through $NC-Fe^{II}_{LS}-CN$ bridges, similar to those linking the Fe^{III} ions in Prussian blue, have also been identified between Mn^{II} ($S = 5/2$),[60] Ni^{II} ($S = 1$),[61] and Mn^{III} ($S = 2$) ions,[62] as they were identified between Ni^{II} ($S = 1$) ions connected by $NC-Co^{III}_{LS}$-CN units.[63] While these reports have implicated diamagnetic metal ions in the exchange coupling of paramagnetic metal sites, to our knowledge, the high field, variable temperature Mössbauer study of cluster **5** presented in this paper gives the first experimental assessment of the electronic spin density at a diamagnetic metal site which is involved in an exchange pathway. Typically, a study of molecules that contain exclusively LS Fe^{II} sites in applied magnetic fields is not necessary, but in the current work it made possible the assessment of the internal field at LS Fe^{II}. At lower applied fields, the internal field induced at LS Fe^{II} would be too small to be measured. Considering this fact, it would be interesting to examine the high-field Mössbauer properties of other compounds in which LS Fe^{II} sites are present within bridges that connect paramagnetic metal ions.[60,61]

Figure 7 depicts the temperature dependence of complex **5**'s thermally averaged spin expectation value, divided by field, calculated for applied fields of 8 and 0.1 T, using a spin Hamiltonian that includes a Heisenberg−Dirac−van Vleck exchange coupling term $-2J\mathbf{S}_{Cr(1)}\cdot\mathbf{S}_{Cr(2)}$ and a Zeeman term $2\mu_B(\mathbf{S}_{Cr(1)}+\mathbf{S}_{Cr(2)})\cdot\mathbf{B}$. Aside from a scaling factor, the curves in Figure 7 accurately describe the temperature dependence of both the internal field at the Fe sites measured at 8 T by Mössbauer spectroscopy and the magnetic susceptibility measured at 0.1 T for $J = 0.65(5)$ cm^{-1}. The 8 T curve in Figure 7 is insensitive to the weak exchange coupling term and represents the saturation behavior of the magnetization of the individual Cr sites. The 0.1 and 8 T curves coincide in the high-temperature regime, where $\langle S\rangle_{th} \approx \chi B$. The fact that the Hamiltonian for the Cr^{III} spins affords a satisfactory description of the spin density at the LS Fe^{II} site indicates that this quantity is induced by the paramagnetic Cr^{III} ions. If we make the reasonable assumption that the electronic spin density induced in the 3d shell of the Fe^{II} site is parallel to the Cr^{III} spins, then the Fermi contact field at the Fe nucleus should be antiparallel to the applied magnetic field, as it is experimentally observed.[66] Given that an unpaired electron in the 3d shell of Fe accounts for a Fermi contact field of ca. −12 T,[64] the internal field induced at the

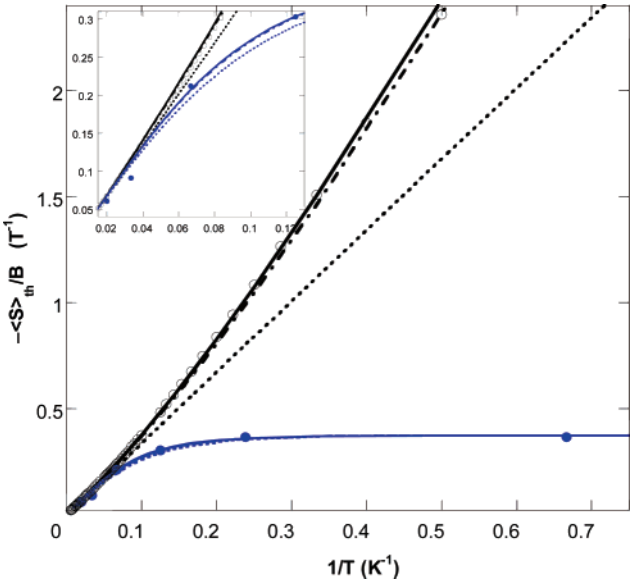

Figure 7. Temperature dependence of the absolute value of the thermally averaged spin expectation value divided by the applied field for cluster **5**, which contains two weakly ferromagnetically coupled $S = {}^3/_2$ metal ions. Black and blue curves represent the values for 0.1 and 8 T, respectively: dotted lines, $J = 0$; broken lines, $J = 0.6$ cm^{-1}; solid lines, $J = 0.7$ cm^{-1}. The temperature dependence of the scaled values for the internal field at Fe^{II} measured at 8 T ($-B_{int}/1.65$) and for magnetic susceptibility ($\chi/1.135$) are also shown in the Figure (blue and black circles, respectively). The scaling factor for B_{int} gives the magnetic hyperfine coupling constant, which is $A = -0.21$ T in $A(\mathbf{S}_{Cr(1)} + \mathbf{S}_{Cr(2)})\cdot\mathbf{I}^{57}_{Fe}$.

Fe^{II} site (−0.6 T) implies an Fe 3d spin population of 0.05 unpaired electrons.

It is important to mention that 30 years ago, Mayoh and Day had formulated a theoretical model to explain the relationship between the Curie temperature of Prussian blue and the partial electron delocalization from Fe^{II} onto the six surrounding Fe^{III} ions, which can be estimated from the intervalence transition band.[6] Taken together with Neel's relation between the Curie temperature and ferromagnetic coupling energy,[65] this model established a relationship between the degree of electron delocalization and the ferromagnetic coupling in Prussian blue. We have developed a theoretical analysis of the mechanism for the exchange coupling between the Cr^{III} ions in the molecular complex **5**, which will be presented in a separate paper to be published in due course.

The series of pentanuclear $[M(tmphen)_2]_3[M'(CN)_6]_2$ clusters exhibit an exceptionally broad range of properties. The cluster with M, M′ = Mn is a single molecule magnet, the analog with M = Co and M′ = Fe exhibits a charge transfer induced spin transition, the Fe^{II} sites in clusters with M = Fe and M′ = Fe or Co undergo temperature induced LS to HS transitions, and the cluster with M = Fe and M′ = Cr displays cyanide linkage isomerism. Several of these properties have been documented for the PB type extended phases based on analogous combinations of transition metal ions while others are specific for molecular compounds. Clearly, this class of cyanide-based

(60) Jiang, L.; Feng, X. L.; Lu, T. B.; Gao, S. *Inorg. Chem.* **2006**, *45*, 5018−5026.
(61) Fukita, N.; Ohba, M.; Okawa, H.; Matsuda, K.; Iwamura, H. *Inorg. Chem.* **1998**, *37*, 842−848.
(62) Egan, L.; Kamenev, K.; Papanikolaou, D.; Takabayashi, Y.; Margadonna, S. *J. Am. Chem. Soc.* **2006**, *128*, 6034−6035.
(63) Chen, X. Y.; Shi, W.; Xia, J.; Cheng, P.; Zhao, B.; Song, H. B.; Wang, H. G.; Yan, S. P.; Liao, D. Z.; Jiang, Z. H. *Inorg. Chem.* **2005**, *44*, 4263−4269.
(64) Gütlich, P.; Link, R.; Trautwein, A. *Mössbauer Spectroscopy and Transition Metal Chemistry*; Springer-Verlag: Berlin, Germany, 1978.
(65) Neél, L. *Ann. Phys.* **1948**, *3*, 137−198.
(66) Fractional, spin-conserving transfer of t_{2g} $3d^\alpha$ electrons from Fe^{II} into the vacant t_{2g} minority spin $3d^\alpha$ orbitals of Cr^{III} yields a net β spin density at the Fe^{II} that is parallel to the majority β spin at the Cr^{III} centers. The Zeeman interaction lowers the energy of the electronic β spins relative to α spins, such that the β electrons are the majority spin carriers in the lowest Zeeman level. This level has the highest Boltzmann population and determines the sign of the internal field.

polynuclear complexes is a promising subject that is worthy of further investigation.

Acknowledgment. K.R.D. acknowledges The National Science Foundation for a PI grant (Grant CHE-0610019) and for equipment grants to purchase the CCD X-ray diffractometer (Grant CHE-9807975) and the SQUID magnetometer (Grant NSF-9974899). C.A. acknowledges Carnegie Mellon University for financial support. Acknowledgment is made to the Donors of the American Chemical Society Petroleum Research Fund for partial support of this research. Prof. Eckard Münck is acknowledged for use of his Mössbauer spectrometers. E.L.B. and S.A.S. acknowledge financial support from NSF award MCB-0424494 to Eckard Münck. We also thank Dr. Andrey Prosvirin for preliminary magnetic measurements on compound **5**. A. D.-A. acknowledges financial support from the Dr. Konrad M. Weis Fellowship in Chemistry (Carnegie Mellon University).

Supporting Information Available: Crystallographic files in CIF format, ORTEP plots of compounds **1**−**5**, Mössbauer spectra of clusters **2** and **5**, results of TGA and mass-spectrometry. This material is available free of charge via the Internet at http://pubs.acs.org.

JA066273X